Original Article
SPATA20 deficiency enhances the metastatic and angiogenic potential of cancer cells by promoting HIF-1α synthesis

Sanga Choi[1,2], Seongkyeong Yoo[1,2], Miyeon Jeon[1,2], Soohyun Park[1,2], Yunsup Choi[1,2], Jiyeon An[1,2], Sungmi Jeon[3], Mingyu Lee[4], Jang-Hyuk Yun[5], Jong-Wan Park[6], Iljin Kim[1,2]

[1]Department of Pharmacology and Program in Biomedical Science and Engineering, Inha University College of Medicine, Incheon 22212, South Korea; [2]Research Center for Controlling Intercellular Communication, Inha University College of Medicine, Incheon 22212, South Korea; [3]Department of Plastic and Reconstructive Surgery, Seoul National University Hospital, Seoul National University College of Medicine, Seoul 03080, South Korea; [4]Division of Allergy and Clinical Immunology, Brigham and Women's Hospital and Department of Medicine, Harvard Medical School, Boston, MA 02115, USA; [5]College of Veterinary Medicine and Institute of Veterinary Science, Kangwon National University, Chuncheon 24341, South Korea; [6]Department of Pharmacology, Seoul National University College of Medicine, Seoul 03080, South Korea

Abstract: Hypoxia-inducible factors (HIFs) regulate cellular oxygen balance and play a central role in cancer metastasis and angiogenesis. Despite extensive research on HIFs, successful therapeutic strategies remain limited due to the intricate nature of their regulation. In this study, we identified SPATA20, a relatively understudied protein with a thioredoxin-like domain, as an upstream regulator of HIF-1α. Depleting SPATA20 induced HIF-1α expression, suggesting a tumor-suppressive role for SPATA20 in cancer cells. SPATA20 depletion increased HIF-1α protein levels and transcriptional activity without affecting its degradation. It appears that SPATA20 inhibits the *de novo* synthesis of HIF-1α, possibly by repressing the cap-dependent translation process involving AKT phosphorylation. Additionally, depletion of SPATA20 promoted cancer cell migration and invasion, which can be reversed by pharmacological inhibition of HIF-1α. Clinical data analysis revealed an inverse correlation between SPATA20 expression and colorectal cancer progression, providing evidence of its role as a potential biomarker. Utilizing SPATA20 as an indicator for HIF-1α-targeting therapy may be an attractive strategy for treating patients with hypoxia-driven cancers. In conclusion, this study demonstrates that SPATA20 deficiency promotes cancer progression by activating the HIF-1α signaling pathway.

Keywords: SPATA20, HIF-1α, hypoxia, cancer

Introduction

Hypoxia-inducible factors (HIFs) are key regulators of cellular oxygen homeostasis [1]. In the context of cancer progression, HIFs play a critical role by regulating the transcriptional activation of genes associated with metastasis and angiogenesis [2, 3]. Despite extensive research efforts aimed at targeting HIFs for cancer therapy, only a limited number of approaches have proven to be successful [4].

HIF proteins are heterodimeric basic helix-loop-helix (bHLH) transcription factors, composed of an α-subunit, which responds to changes in oxygen levels, and a β-subunit (also known as aryl hydrocarbon receptor nuclear translocator, ARNT), which is expressed constitutively [5-7]. Under normal oxygen conditions (referred to as normoxia), HIF-α is hydroxylated at conserved proline residues by HIF prolyl hydroxylases (PHDs) [7]. Subsequently, the von Hippel-Lindau tumor suppressor (VHL), an E3 ubiquitin ligase, binds to hydroxylated HIF-α, inducing its proteasomal degradation through ubiquitination [8]. However, in hypoxic conditions, HIF-α undergoes stabilization and translocation to the nucleus. In the nucleus, it associates with its heterodimeric partner, HIF-β, forming an active transcriptional complex. This complex then

binds to hypoxia-responsive elements (HREs) located in the promoter or enhancer region of target genes, resulting in their transactivation [6, 9].

Previous studies have found that HIF-1 interacts with a class of small redox proteins, leading to crosstalk between hypoxic response and cellular redox homeostasis [10-17]. Spermatogenesis-associated protein 20 (SPATA20) is a relatively understudied protein that contains a conserved thioredoxin-like domain at the N-terminal region, which includes a characteristic CXXC motif that may act as a potential catalytic site for the redox regulation of substrates [18]. SPATA20 is aberrantly expressed in the testis and involved in the development and maturation of sperm [18-21]. Recent proteomic and whole-exome sequencing (WES) studies have suggested its potential role in colorectal cancer, although its exact function remains unclear [22, 23].

In this study, we identified SPATA20 as a novel upstream regulator of HIF-1α. Our investigations revealed that depleting SPATA20 increases both the protein abundance and transcriptional activity of HIF-1α. These findings shed light on the tumor-suppressive function of SPATA20 in cancer cells, thereby providing evidence for the potential therapeutic use of HIF inhibitors in treating patients affected by hypoxia-driven cancers with low levels of SPATA20 expression.

Materials and methods

Cell culture

Human colon cancer (DLD-1 and HCT116), and liver cancer (Hep3B) cell lines were obtained from the American Type Culture Collection (ATCC, Manassas, VA). Human kidney cancer (SNU-349) and Tera-1 testicular cell lines was obtained from the Korean Cell Line Bank (Seoul, South Korea). Human umbilical vein endothelial cells (HUVECs) were purchased from PromoCell (Heidelberg, Germany). Human Sertoli cells (HSerCs) were purchased from ScienCell Research Laboratories (Carlsbad, CA). Cell culture reagents were purchased from GenDEPOT (Katy, TX), unless otherwise specified. DLD-1, HCT116, SNU-349, and Tera-1 cells were cultured in RPMI complemented with 10% heat-inactivated fetal bovine serum (FBS) and 1% penicillin-streptomycin. Hep3B cells were

cultured in DMEM. HUVECs were cultured in endothelial cell growth medium with a supplement mixture (PromoCell). HSerCs were cultured in Sertoli cell medium with a supplement mixture (ScienCell Research Laboratories). The cells were maintained under standard conditions of 37°C and 5% CO_2 in a humidified atmosphere. For hypoxic challenge, cells were incubated in a hypoxia chamber (Memmert, Schwabach, Germany) set to an oxygen concentration of 1%.

Plasmids and siRNAs

Plasmid DNA constructs encoding SPATA20 or SPATA20 shRNA were purchased from OriGene (Rockville, MD). EPO- and VEGF-luciferase plasmids were constructed as described previously [24, 25]. The plasmids were verified through standard DNA sequencing. Small interfering RNAs (siRNAs) were obtained from IDT (Coralville, IA) and Bioneer (Daejeon, South Korea), and their sequences are listed in Supplementary Table 1. Plasmids and siRNAs were transfected using jetPRIME (Polyplus, Illkirch-Graffenstaden, France) and RNAiMAX (Thermo Fisher Scientific, Waltham, MA) reagents, respectively, following the manufacturer's instructions.

Reagents and antibodies

Dimethyloxalylglycine (DMOG) and MG132 were purchased from MedChemExpress (Monmouth Junction, NJ). Cycloheximide was purchased from Merck (Darmstadt, Germany). The antibodies used in this study include anti-SPATA20 (HPA031442) from Merck, anti-GFP (#2956), anti-AKT (#9272), and anti-phospho-AKT (#9271) from Cell Signaling Technology (Danvers, MA), and anti-α-tubulin (sc-5364) and anti-β-tubulin (sc-9104) from Santa Cruz Biotechnology (Dallas, TX). The anti-HIF-1α antibody was raised in a rabbit, as previously described [26].

Enzyme-linked immunosorbent assay (ELISA)

A HIF-1α sandwich ELISA kit (Thermo Fisher Scientific) was used according to the manufacturer's instructions. The ELISA microplates were loaded with standards and samples, and then placed on a shaker at room temperature for a 2-hour incubation period. Subsequently, the wells were washed three times before the addition of biotinylated detection antibodies to

each well. After a 1-hour incubation, the wells were washed three times to eliminate unbound antibodies. Streptavidin-HRP was added to each well, and the plate was incubated for 30 minutes. After washing the wells three times, TMB substrates were added to each well and the plates were further incubated for 30 minutes in the dark. The enzymatic reaction was stopped by the addition of a stop solution, and the absorbance at a wavelength of 450 nm was measured using a microplate reader.

Western blot analysis

Protein samples were boiled in SDS sample buffer at 95°C for 5 to 10 minutes. The denatured proteins were then separated by SDS-PAGE and transferred onto an Immobilon-P membrane (Merck). The membrane was blocked with 5% skim milk and probed with the specified primary antibodies. Secondary antibodies were applied, and the bands were visualized using ECL Western substrates (Enzynomics, Daejeon, South Korea).

Luciferase reporter assay

The luciferase assay was conducted using the EZ luciferase assay system (Enzynomics). Cells were transfected with the specified reporter plasmids and subsequently lysed with luciferase lysis buffer. The resulting lysates were then mixed with a reaction buffer containing substrates, and the luciferase activities were analyzed using the Victor X Light luminescence plate reader (PerkinElmer, Waltham, MA). β-galactosidase activities were measured to normalize for transfection efficiency.

Quantitative reverse transcription PCR (RT-qPCR)

Total RNA was isolated using TRIzol reagent (Thermo Fisher Scientific), and cDNA synthesis was carried out with the M-MLV cDNA synthesis kit (Enzynomics). RT-qPCR was performed on 96-well optical plates using the qPCR mastermix (Enzynomics). The expression levels of the target genes were determined relative to the expression of *ACTB*. qPCR primer sequences are provided in Supplementary Table 2.

Immunoprecipitation (IP)

Cells were lysed using IP buffer supplemented with protease and phosphatase inhibitors (GenDEPOT). After clearing the cell debris via centrifugation, the remaining lysates were incubated with the indicated antibodies at 4°C with slow rotation overnight. Subsequently, protein A/G-conjugated beads from Bio-Rad Laboratories (Hercules, CA) were added and incubated for an additional hour. The precipitates were washed three times and then resuspended in sample buffer.

Conditioned media preparation

Cells were placed in serum-free media containing antibiotics before being cultured under either hypoxia or 1 mM DMOG for 24 hours. The conditioned media were retrieved and subsequently subjected to centrifugation at room temperature for 3 minutes. The resulting supernatants were filtered through a syringe filter with a diameter of 0.45 μm and stored at -20°C until they were used for downstream analysis.

Transwell assays

Transwell migration and invasion assays were conducted using permeable inserts (8 μm pore size) purchased from Corning (Corning, NY). For the invasion assay, the inserts were coated with growth factor-reduced basement membrane extract (BME) obtained from R&D Systems (Minneapolis, MN). The cells were seeded onto the upper chambers in serum-free medium, while the lower chambers were filled with medium containing FBS, and then incubated under hypoxic conditions or treated with 1 mM DMOG for 24 hours. The cells located on the lower surface of the transwell insert were fixed using a 4% paraformaldehyde solution and subsequently stained with H&E. Cells from five random fields of each membrane were counted using a microscope.

Tube formation assay

Tube formation assay was conducted using the Cultrex in vitro angiogenesis assay kit, which was purchased from R&D Systems. Passage 3-4 HUVECs were suspended in the conditioned media and then seeded in a 96-well plate coated with growth factor-reduced BME. After a 6-hour incubation period, the cells were treated with a 2 μM Calcein AM solution. Tube formation was assessed using fluorescence microscopy, and the number of branch points, junctions, and tube lengths were analyzed using ImageJ software.

Analysis of public database

Clinical data of patients with colorectal cancer were obtained from publicly available databases, including the International Cancer Genome Consortium (ICGC), The Cancer Genome Atlas (TCGA), the Genotype-Tissue Expression (GTEx), and the Gene Expression Omnibus (GEO). Gene alteration frequency was analyzed using the cBioPortal platform. Differential analysis of RNA-seq and gene chip data was performed on the TNMplot platform.

Tissue microarray analysis

Tissue microarray comprised of human colorectal cancer and normal tissues was purchased from SuperBioChips Laboratories (Seoul, South Korea). The array slide was subjected to a 1-hour drying process at 60°C, followed by autoclaving the dewaxed slide in an antigen retrieval agent and subsequent treatment with 3% hydrogen peroxide. Primary antibodies were used overnight at 4°C, followed by the application of biotinylated secondary antibodies at room temperature for 1 hour on the next day. A peroxidase-based detection system was used to visualize the resulting immune complex. Each tissue core was evaluated by multiplying the staining intensity by the percentage of positive cells.

Statistical analysis

The data analysis was conducted using Excel and Prism 9 software. The experimental results are presented as means with their corresponding standard deviations (SDs). Statistical significance was determined based on a *p*-value of less than 0.05.

Results

Depletion of SPATA20 increases the protein levels of HIF-1α

Previous studies have shown that redox proteins, such as thioredoxins, can interact with HIF-1α, thereby controlling its stability and activity [15, 27]. To identify potential candidates, we selected the top 20% of the 127 proteins classified as thioredoxin-like fold proteins based on their co-expression with HIF-1α in the ICGC/TCGA pan-cancer study [28]. These candidates were then subjected to an ELISA-based siRNA screening (**Figure 1A**). Within the pool of candidates, the depletion of SPATA20 led to a significant increase in the HIF-1α protein level. This finding was further validated by depleting SPATA20 using two different siRNAs (Supplementary Figure 1A and 1B) in both human tumor cells and normal testis cells exposed to hypoxia (**Figure 1B** and **1C**, Supplementary Figure 2A and 2B) or treated with DMOG (**Figure 1D** and **1E**, Supplementary Figure 2C and 2D), which is a hypoxia mimetic agent that inhibits the 2-oxoglutarate (2-OG)-dependent hydroxylation of HIF-1α, leading to the stabilization of the HIF-1α protein [29]. Furthermore, the knockdown of SPATA20 in *VHL*-mutant SNU-349 cells, which express HIF-1α under normoxia, also led to an elevation in HIF-1α protein levels (**Figure 1F**). These data demonstrate that the depletion of the thioredoxin-like protein SPATA20 increases the protein levels of HIF-1α.

Depletion of SPATA20 activates HIF-1α and induces its target gene expression

To evaluate the effect of SPATA20 on HIF-1α transcriptional activity, we utilized luciferase reporter plasmids containing the HRE sequence of the *EPO* enhancer. This sequence is a well-known HIF target. When the transcription factor HIF-1α binds to the EPO HRE sequence, it leads to an increase in luciferase activity, which reflects the upregulation of HIF-1α expression. Under hypoxic conditions, knockdown of SPATA20 increased the activity of HIF-1α on EPO-luciferase (**Figure 2A**, Supplementary Figure 3A), while it did not affect the activity on the mutant form of EPO-luciferase, which is unable to bind to HIF-1α due to a mutation in the HRE region. These findings were further validated in cells treated with DMOG (**Figure 2B**, Supplementary Figure 3B). We also utilized another luciferase reporter plasmid harboring an HRE from the *VEGF* promoter. Similarly, VEGF-luciferase activity was enhanced by SPATA20 depletion under hypoxic and hypoxia-mimetic conditions (**Figure 2C** and **2D**). Furthermore, to assess the effects of SPATA20 on HIF-1α target genes, we measured the mRNA expression levels of plasminogen activator urokinase (*PLAU*), endothelin 1 (*EDN1*), heme oxygenase 1 (*HMOX1*), and adrenomedullin (*ADM*) (**Figure 2E-H**, Supplementary Figure 3C-F). SPATA20 knockdown resulted in up-
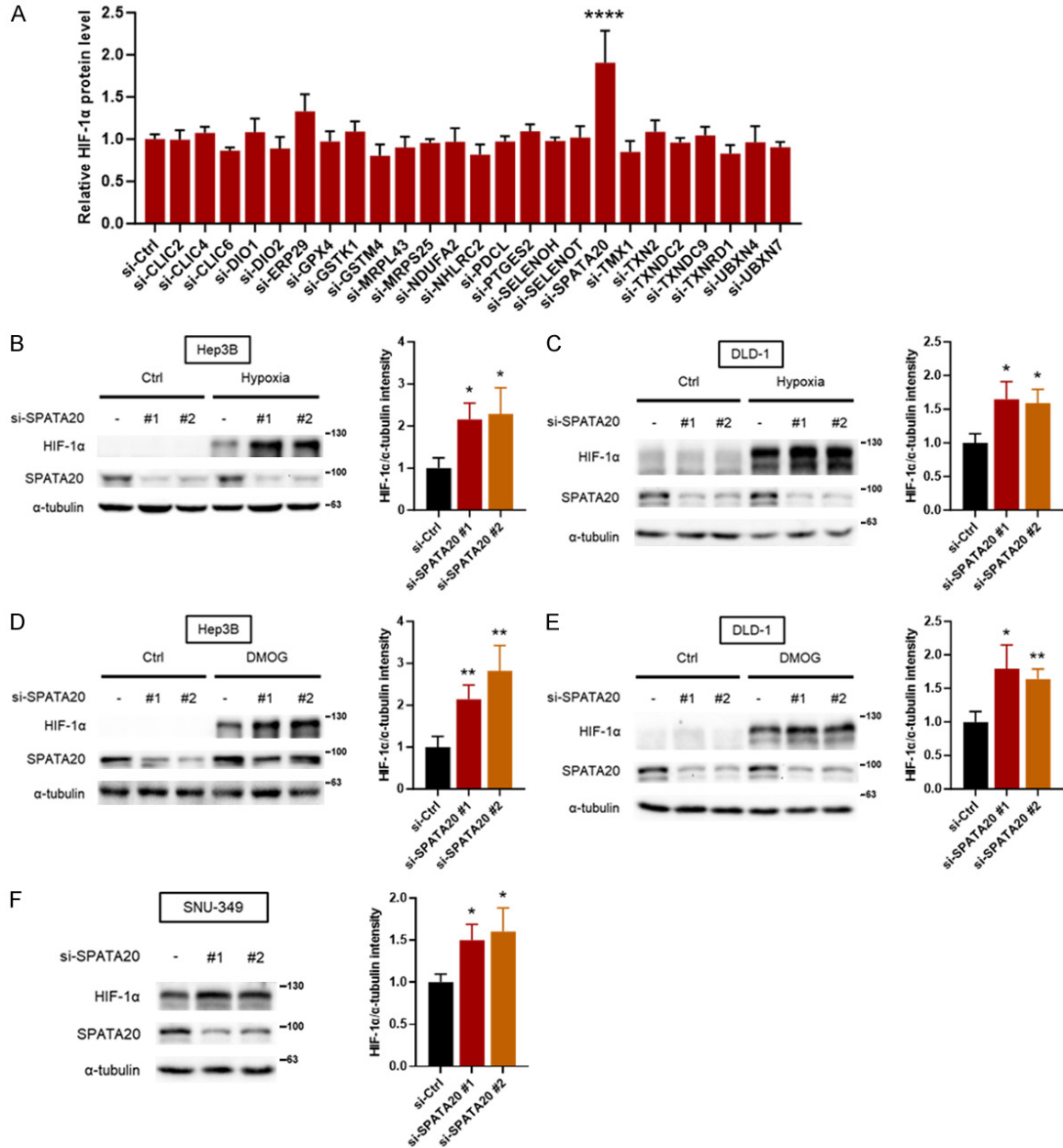
Figure 1. SPATA20 knockdown increases HIF-1α protein levels. (A) Hep3B cells were transfected with the indicated siRNAs and lysed for analysis using an HIF-1α sandwich ELISA kit. Quantification of HIF-1α protein levels is presented as means and SDs (n = 3). ****$P < 0.0001$ compared to the si-Ctrl group by one-way ANOVA. (B-E) Hep3B and DLD-1 cells were transfected with indicated siRNAs and incubated in hypoxia (B, C) or treated with 1 mM DMOG (D, E) for 8 hours. Cell lysates were analyzed by Western blotting with the indicated antibodies. The bar graphs display the band intensities of HIF-1α protein normalized to the intensities of α-tubulin in the hypoxia or DMOG groups. Data are presented as means and SDs (n = 3). *$P < 0.05$ and **$P < 0.01$ compared to the si-Ctrl groups by Student's t-test. (F) *VHL*-mutant SNU-349 cells were transfected with indicated siRNAs and subjected to Western blotting. Data are presented as means and SDs (n = 3). *$P < 0.05$ by Student's t-test.

regulated expression of proangiogenic genes. Collectively, these data indicate that SPATA20 depletion results in HIF-1α activation, thereby inducing the transcription of its downstream genes.

Restoration of SPATA20 suppresses HIF-1α in cells depleted of SPATA20

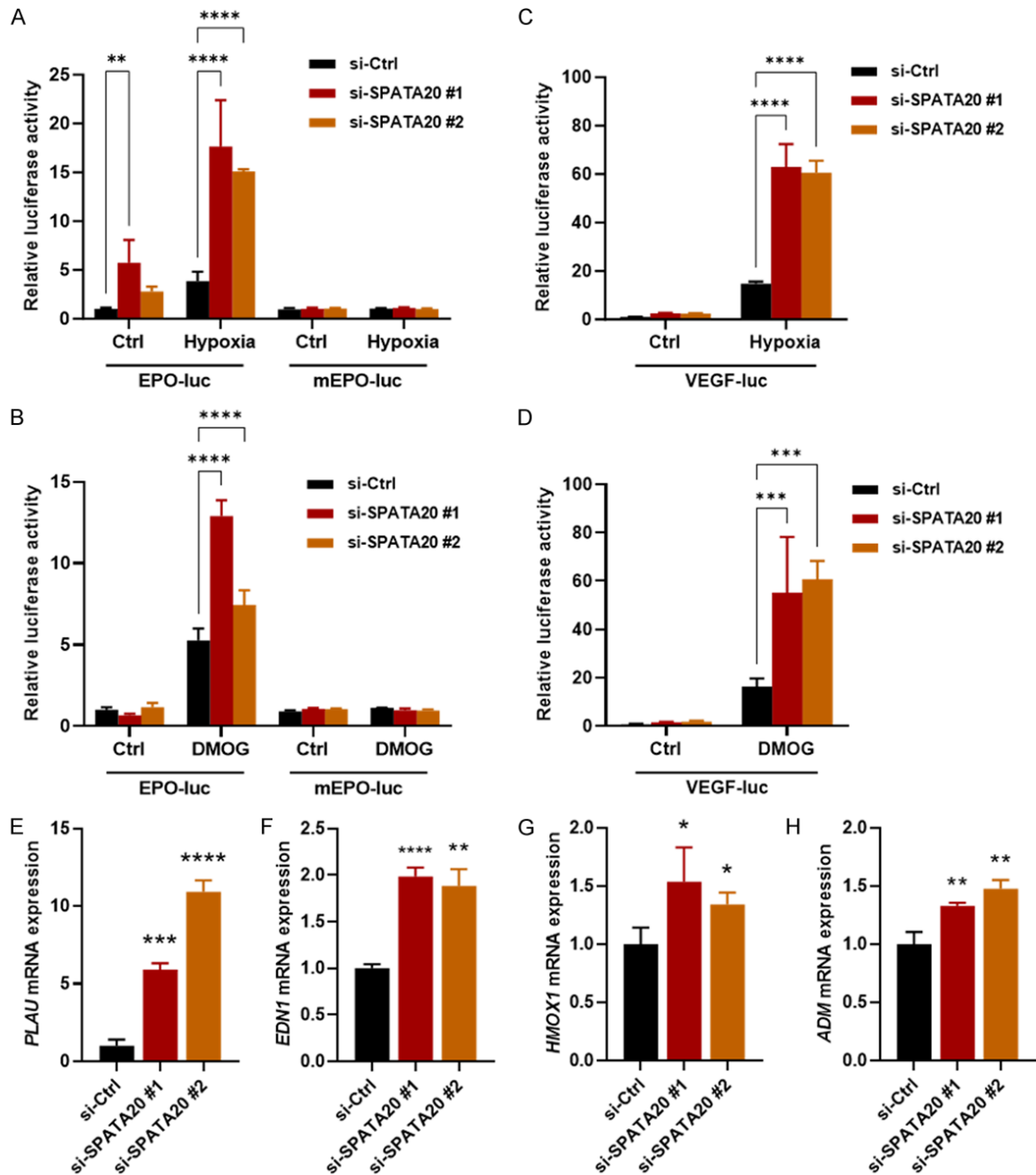Meanwhile, ectopic expression of SPATA20 did not significantly change the protein levels of

Figure 2. SPATA20 knockdown activates HIF-1α and induces the expression of HIF-1α target genes. (A, B) Hep3B cells expressing EPO-luciferase plasmids were transfected with the indicated siRNAs and then incubated in hypoxia (A) or treated with 1 mM DMOG (B) for 24 hours. Cells were lysed and subjected to the luciferase assay. (C, D) Cells were transfected with VEGF-luciferase and indicated siRNAs and then incubated in hypoxia (C) or treated with 1 mM DMOG (D) for 24 hours. Cells were lysed and subjected to luciferase assay. β-galactosidase activities were measured to normalize for transfection efficiency. Data represents the mean ± SD (n = 3). $**P < 0.01$, $***P < 0.001$ and $****P < 0.0001$ by two-way ANOVA. (E-H) Cells were transfected with indicated siRNAs and cultured in hypoxia for 24 hours. Cells were lysed for RNA extraction, and the mRNA expression levels of *PLAU* (E), *EDN1* (F), *HMOX1* (G), and *ADM* (H) were measured by RT-qPCR. Relative expression levels were determined by normalizing to *ACTB* expression levels. Data represents the mean ± SD (n = 3). $*P < 0.05$, $**P < 0.01$, $***P < 0.001$, and $****P < 0.0001$ compared to the si-Ctrl groups by Student's t-test.

HIF-1α under hypoxia or DMOG (Supplementary Figure 4A-C). Similarly, the overexpression of SPATA20 in *VHL*-mutant SNU-349 cells likewise had no effect on the levels of HIF-1α protein (Supplementary Figure 4D). Furthermore, SPATA20 overexpression had no effect on
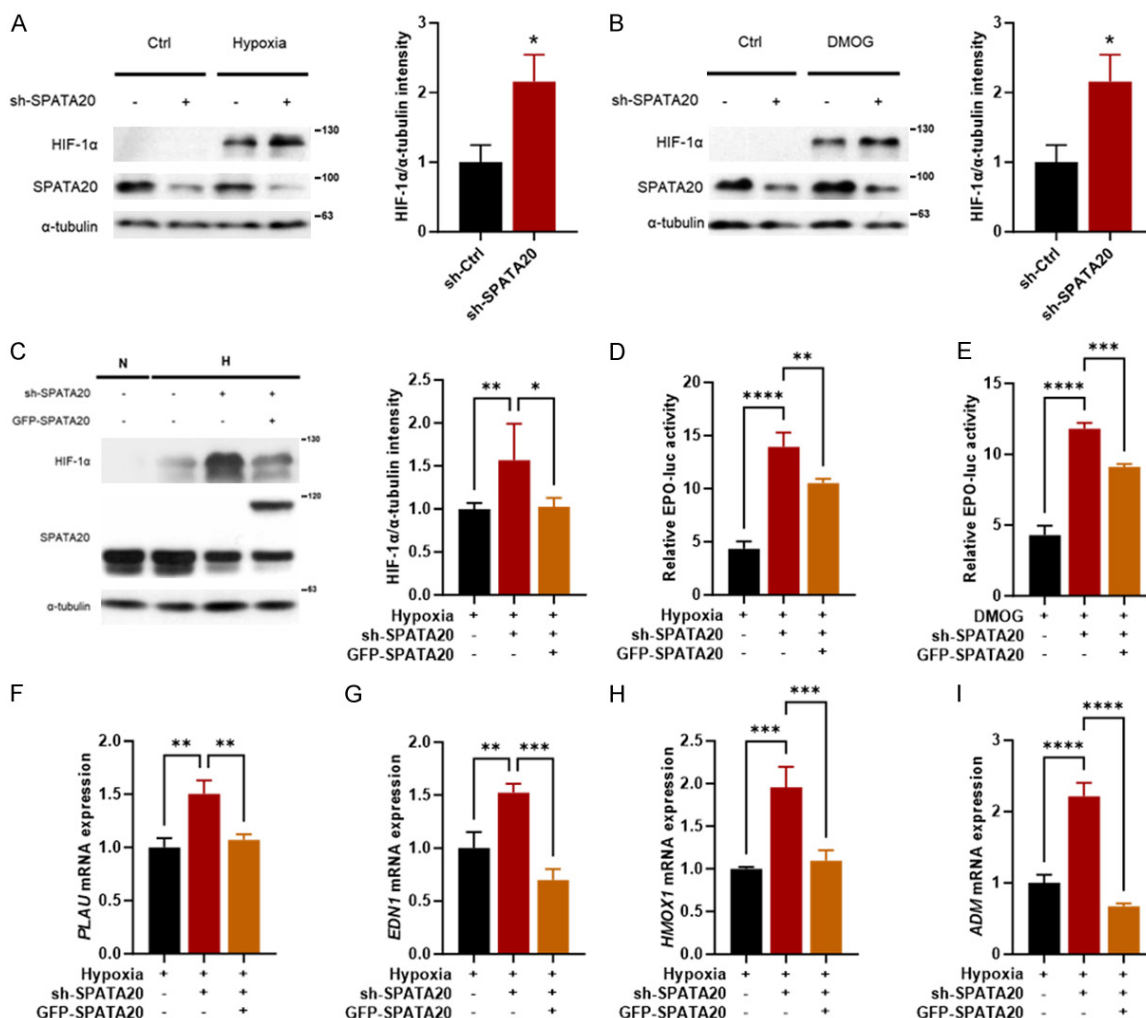
Figure 3. Restoration of SPATA20 reverses the HIF-1α activation induced by SPATA20 knockdown. (A, B) DLD-1 cells were depleted of SPATA20 with lentiviral SPATA20 shRNA. Cells were incubated in hypoxia (A) or treated with 1 mM DMOG (B) for 8 hours. Cell lysates were analyzed by Western blotting with the indicated antibodies. The bar graphs display the band intensities of HIF-1α protein normalized to the intensities of α-tubulin in the hypoxia or DMOG groups. Data are presented as means and SDs (n = 3). *P < 0.05 and **P < 0.01 by Student's t-test. (C) SPATA20 knockdown cells were transfected with GFP-SPATA20 and incubated in hypoxia for 8 hours. Cell lysates were analyzed by Western blotting. Data are presented as means and SDs (n = 5). *P < 0.05 by one-way ANOVA. (D, E) Cells were transfected with EPO-luciferase and indicated plasmids and then incubated in hypoxia (D) or treated with 1 mM DMOG (E) for 24 hours. Cells were lysed and subjected to luciferase assay. β-galactosidase activities were measured to normalize for transfection efficiency. Data represents the mean ± SD (n = 3). **P < 0.01, ***P < 0.001 and ****P < 0.0001 by two-way ANOVA. (F-I) Cells were transfected with indicated plasmids and cultured in hypoxia for 24 hours. Cells were lysed for RNA extraction, and the mRNA expression levels of *PLAU* (F), *EDN1* (G), *HMOX1* (H), and *ADM* (I) were measured by RT-qPCR. Relative expression levels were determined by normalizing to *ACTB* expression levels. Data represents the mean ± SD (n = 3). **P < 0.01, ***P < 0.001, and ****P < 0.0001 by two-way ANOVA.

either the *HIF1A* mRNA or pre-mRNA expression levels (Supplementary Figure 4E and 4F). To address this issue, we established a SPATA20-depleted cell line that was stably transfected with a lentiviral SPATA20 shRNA vector. shRNA-mediated depletion of SPATA20 increased the protein levels of HIF-1α under hypoxic or DMOG-treated conditions (**Figure 3A** and **3B**). Ectopic re-expression of SPATA20 in these cells successfully inhibited HIF-1α protein levels (**Figure 3C**). In EPO-luciferase assays, the re-expression of SPATA20 reversed the activating effects of SPATA20 depletion on HIF-1α transcriptional activity (**Figure 3D** and
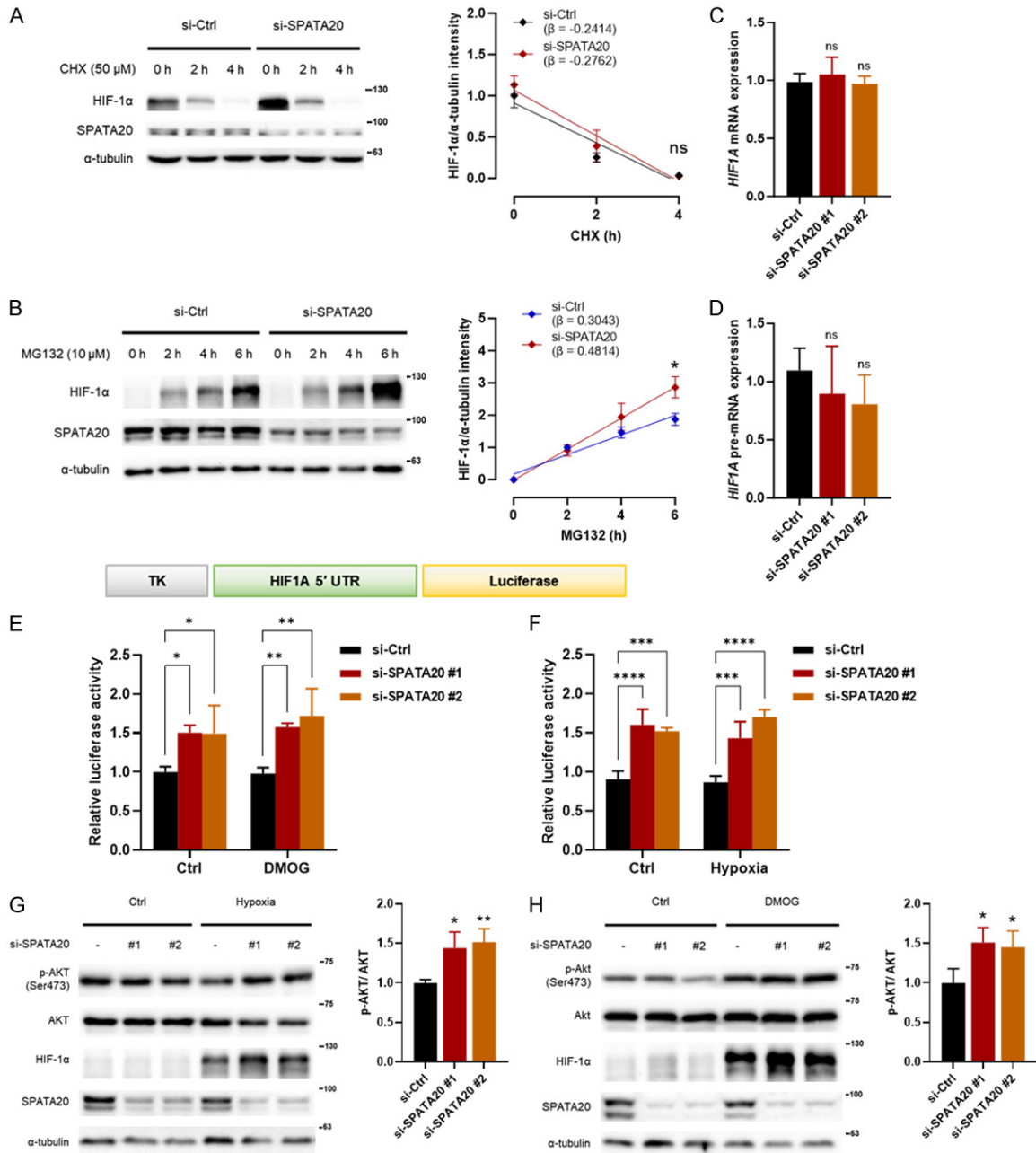
Figure 4. SPATA20 knockdown increases the cap-dependent translation of HIF-1α. (A) Hep3B cells were transfected with indicated siRNAs and treated with 1 mM DMOG for 8 hours followed by 50 µM cycloheximide (CHX) treatment for indicated time periods. Cells were lysed and subjected to Western blotting. The band intensities of HIF-1α protein were normalized to the intensities of α-tubulin. Relative band intensities to the non-CHX-treated groups were displayed as line graphs at the right panel with calculated slope values (β). Data are presented as means and SDs (n = 3). ns, non-significant ($P > 0.05$ by Student's t-test). (B) Cells were transfected with indicated siRNAs and treated with 10 µM MG132 for indicated time periods. Relative band intensities to the non-MG132-treated groups were displayed as line graphs at the right panel with calculated slope values (β). *$P < 0.05$ by Student's t-test. (C, D) Cells were transfected with indicated siRNAs and lysed for RNA extraction. *HIF1A* mRNA (C) and *HIF1A* pre-mRNA (D) expression levels were measured by RT-qPCR. ns, non-significant ($P > 0.05$ by Student's t-test). (E, F) Cells were transfected with *HIF1A* 5' UTR-luciferase plasmid and indicated siRNAs and then incubated in hypoxia (E) or treated with 1 mM DMOG (F) for 24 hours. The structure of the luciferase reporter plasmid containing the 5' UTR region of *HIF1A* mRNA is displayed in the top panel. Cells were lysed and subjected to luciferase assay. β-galactosidase activities were measured to normalize for transfection efficiency. Data are presented as means and SDs (n = 3). *$P < 0.05$, **$P < 0.01$, ***$P < 0.001$, and ****$P < 0.0001$ by two-way ANOVA. (G, H) Cells were transfected with indicated siRNAs and then incubated in hypoxia or treated with 1 mM DMOG for 8 hours. Cell lysates were analyzed by Western blotting with the indicated antibodies. The bar graphs display the band intensities of phospho-AKT normalized to the intensities of total AKT in the hypoxia and DMOG groups. Data are presented as means and SDs (n = 3). *$P < 0.05$ compared to the si-Ctrl groups by Student's t-test.
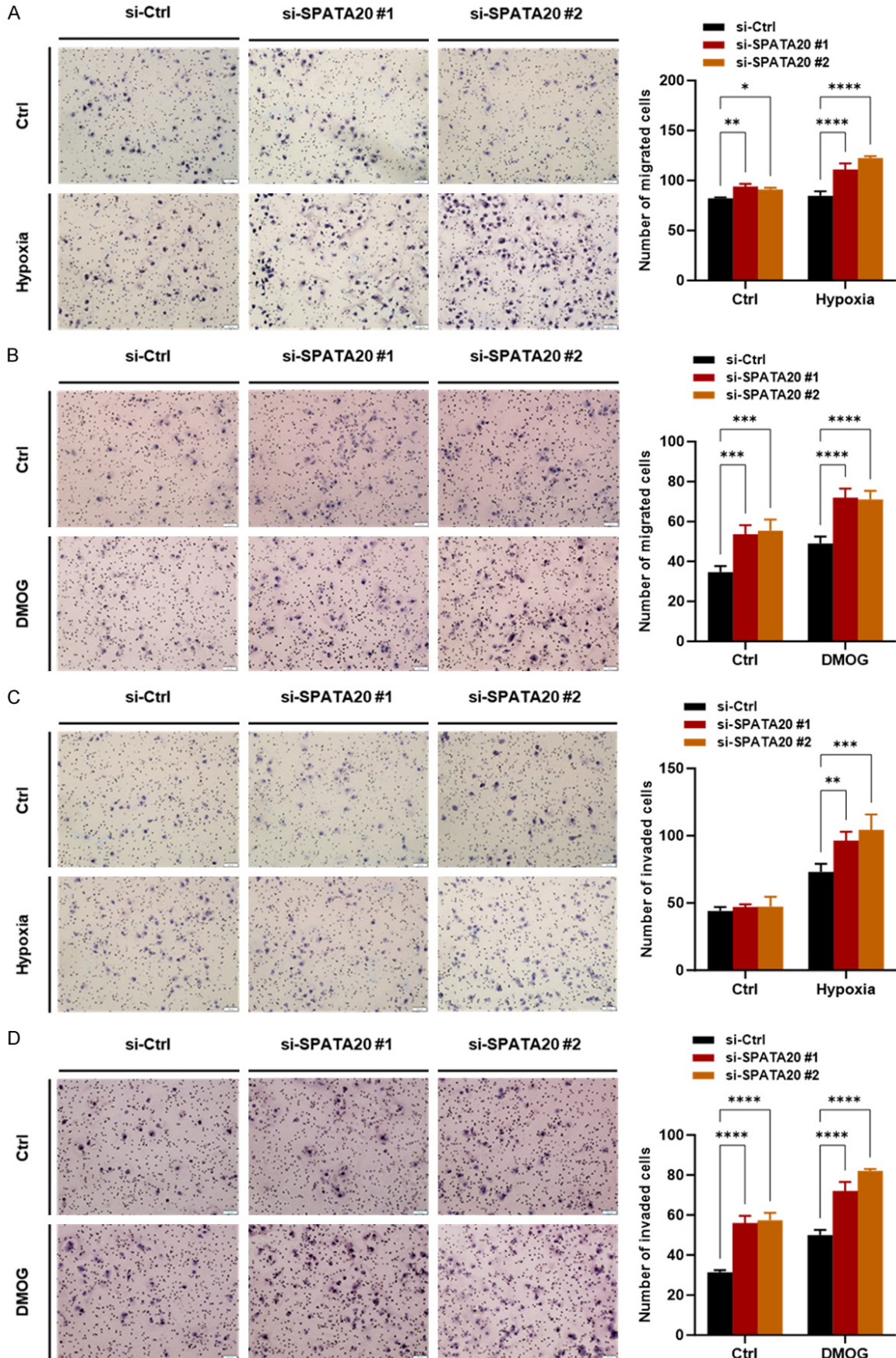
Figure 5. SPATA20 knockdown promotes the migration and invasion of cancer cells. (A, B) HCT116 cells were transfected with indicated siRNAs and subjected to transwell migration assays under hypoxia (A) or with 1 mM DMOG (B) added to the lower chambers. Representative images of migrated cells are shown. The scale bars represent 100 μm. The average number of migrated cells was calculated from five random microscopic fields. (C, D) Cells were transfected with indicated siRNAs and subjected to invasion assays under hypoxia (C) or with 1 mM DMOG (D) added to the lower chambers. Representative images of invaded cells are shown. The average number of invaded cells was calculated from five random microscopic fields. Data are presented as means and SDs (n = 3). *$P < 0.05$, **$P < 0.01$, ***$P < 0.001$, and ****$P < 0.0001$ by two-way ANOVA.

3E). Similarly, SPATA20 re-expression counteracted the effects of SPATA20 depletion on HIF-1α target genes (**Figure 3F-I**). These findings suggest that SPATA20 may require additional interacting partners to efficiently regulate HIF-1α, and further studies are needed to clarify the underlying mechanisms.

Depletion of SPATA20 enhances HIF-1α synthesis

Given the potential role of SPATA20 in mediating redox reactions, we conducted an IP assay to investigate the possible protein-protein interaction between HIF-1α and SPATA20. However, the IP results did not provide any evidence of a direct interaction between the two proteins (Supplementary Figure 5). Subsequently, we investigated the mechanism by which SPATA20 regulates HIF-1α expression. To evaluate whether SPATA20 decreases HIF-1α protein levels through degradation, we analyzed the degradation rate of HIF-1α by initially treating cells with DMOG to stabilize HIF-1α, followed by treating the cells with cycloheximide (CHX), a translation inhibitor (**Figure 4A**). No significant difference was found in the degradation rate of HIF-1α between the control group and the SPATA20 knockdown group. This suggests that SPATA20 does not regulate HIF-1α protein through proteasomal degradation. Meanwhile, the accumulation rate of HIF-1α increased when cells were treated with MG132, a proteasome inhibitor (**Figure 4B**). As a result, we anticipated that SPATA20 may control the transcription or translation of HIF-1α. We performed RT-qPCR to assess the expression of HIF1A mRNA and pre-mRNA, but no significant differences were observed between the control group and the SPATA20 knockdown group (**Figure 4C** and **4D**). Since the transcription of HIF-1α did not show an increase with SPATA20 knockdown, we proceeded to investigate whether SPATA20 governs the translation of HIF-1α. We utilized a luciferase reporter plasmid containing the 5' untranslated region (5' UTR) region of *HIF1A*

mRNA, which replicates the cap-dependent translation of HIF-1α. The luciferase activity was observed to be enhanced by SPATA20 knockdown in both normoxia and hypoxia, as well as with DMOG treatment (**Figure 4E** and **4F**). Furthermore, since the translation of HIF-1α is regulated by the protein kinase B (AKT) pathway [30], we analyzed the activation status of AKT following the depletion of SPATA20 (**Figure 4G** and **4H**). Notably, the knockdown of SPATA20 resulted in elevated expression of the active, phosphorylated form of AKT (Ser 473) under both hypoxic and DMOG-treated conditions. In conclusion, these findings suggest that the depletion of SPATA20 enhances the synthesis of HIF-1α protein.

Depletion of SPATA20 promotes the migration and invasion of hypoxic cancer cells

The unfavorable prognosis of cancer can be attributed to the metastatic potential of tumor cells [31, 32]. Given the critical role of HIF-1α in hypoxia-induced cancer metastasis [33, 34], we focused on examining the effects of SPATA20 on cell migration. Transwell assays were conducted to evaluate the migratory and invasive properties of cells. SPATA20 siRNAs increased the migratory ability of HCT116 cells under hypoxic conditions (**Figure 5A**). Likewise, the knockdown of SPATA20 in DMOG-treated conditions resulted in an increased number of migrated cells (**Figure 5B**). In transwell invasion assays, SPATA20 knockdown promoted cell invasion in both hypoxic and DMOG-treated conditions (**Figure 5C** and **5D**). Similar results were observed in Hep3B cells as well (Supplementary Figure 6A-D). Next, we examined whether inhibiting HIF-1α could reverse the pro-migratory and pro-invasive effects induced by SPATA20 depletion. We treated cancer cells with YC-1, an HIF-1α inhibitor, and observed its dose-dependent suppression of the migration/invasion of SPATA20-depleted cells under hypoxic (**Figure 6A** and **6C**) and DMOG-treated conditions (**Figure 6B** and **6D**).
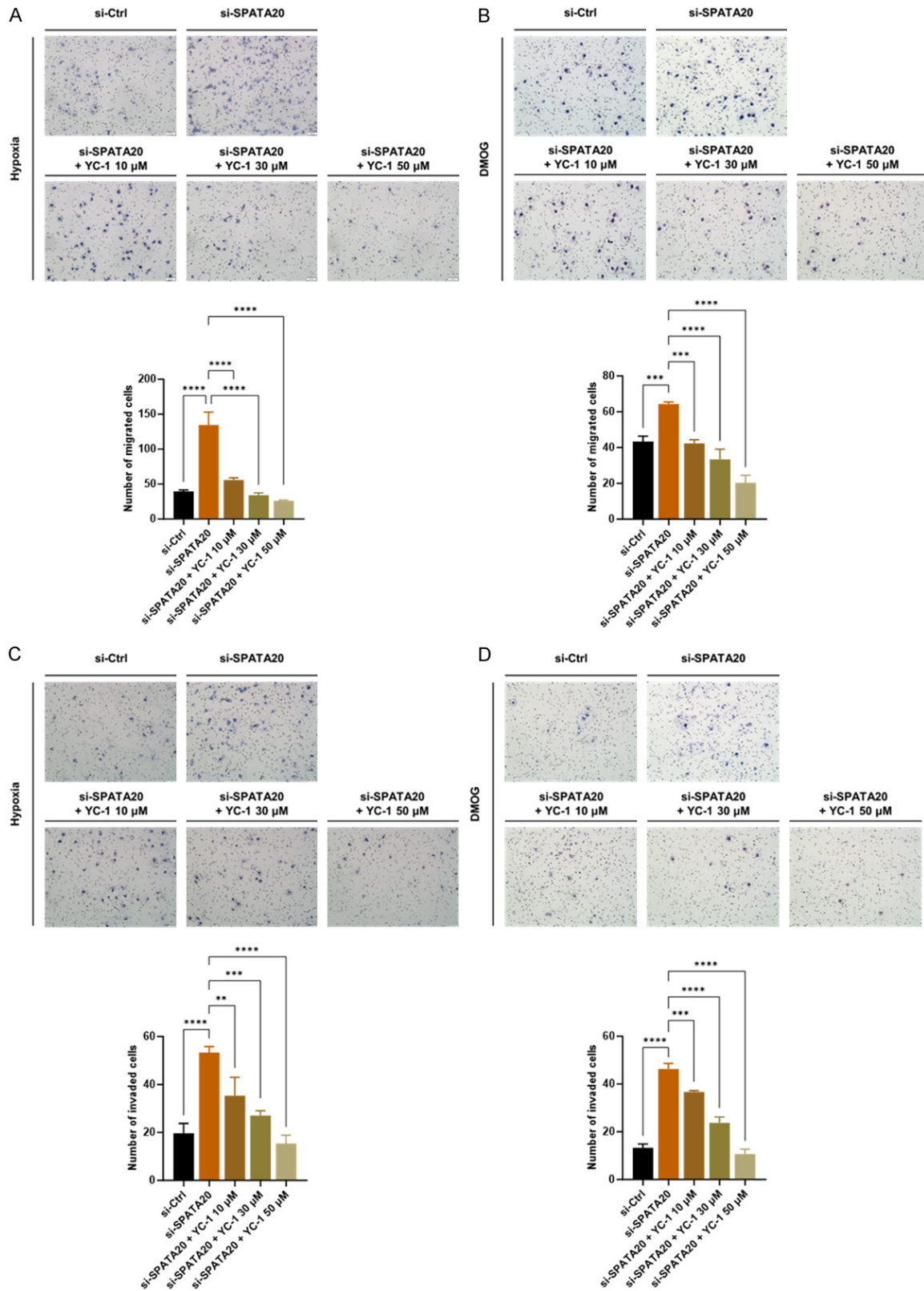
Figure 6. Inhibition of HIF-1α by YC-1 abrogates the pro-migratory and invasive effects induced by SPATA20 knock-down (A, B) HCT116 cells were transfected with indicated siRNAs and subjected to transwell migration assays under hypoxia (A) or with 1 mM DMOG (B) added to the lower chambers. YC-1 was added at specified doses. Representative images of migrated cells are shown. The average number of migrated cells was calculated from five random

microscopic fields. The scale bars represent 100 μm. (C, D) Cells were transfected with indicated siRNAs and subjected to invasion assays under hypoxia (C) or with 1 mM DMOG (D) added to the lower chambers. YC-1 was added at specified doses. Representative images of invaded cells are shown. The average number of invaded cells was calculated from five random microscopic fields. Data are presented as means and SDs (n = 3). $*P < 0.05$, $**P < 0.01$, $***P < 0.001$, and $****P < 0.0001$ by one-way ANOVA.

In summary, the depletion of SPATA20 accelerates hypoxic cell migration and invasion, suggesting that SPATA20-deficient cancer cells are more prone to enhancing their metastatic potential mediated by HIF-1α.

Depletion of SPATA20 promotes the angiogenic potential of endothelial cells

Since it is well known that angiogenesis is activated by hypoxia [35], we examined the motility of endothelial cells to evaluate the effect of SPATA20 on angiogenesis. In transwell migration assays, HUVECs were cultured in conditioned media collected from SPATA20-depleted cancer cells grown under hypoxic or DMOG-treated conditions. In both conditions, the number of migrated cells in the SPATA20 knockdown groups was significantly higher when compared to the control groups (**Figure 7A** and **7B**). Similarly, in transwell invasion assays, the invasion of HUVECs was facilitated by SPATA20 knockdown in both hypoxia and DMOG (**Figure 7C** and **7D**). Subsequently, in order to evaluate the effects of SPATA20 knockdown on the tube formation ability of endothelial cells, we performed an *in vitro* tube formation assay utilizing HUVECs. The results demonstrated an increase in the formation of a vascular network in the SPATA20 knockdown groups compared to the control groups. The SPATA20 knockdown groups exhibited a higher number of junctions and branches, as well as an increased total tube length (Supplementary Figure 7A-D). These findings, along with the RT-qPCR results (**Figure 2E-H**), provide further evidence that the depletion of SPATA20 enhances the angiogenic potential of endothelial cells by upregulating HIF-1α downstream pro-angiogenic factors.

Downregulation of SPATA20 is associated with poor prognosis in patients with colorectal cancer

A previous study reported that genetic variants of SPATA20 were detected in the WES of patients with early-onset colorectal cancer [23]. To investigate the clinical implications of SPATA20 in colorectal cancer, publicly available datasets from multiple institutions were analyzed using the cBioPortal database. In accordance with the WES data, several mutations of SPATA20 were detected in a small subset of patient populations (**Figure 8A**). Moreover, SPATA20 expression levels were compared between normal and tumor tissues to assess the potential association of SPATA20 with disease development. In the TCGA/GTEx datasets, *SPATA20* mRNA expression was downregulated in tumor tissues compared to normal tissue (**Figure 8B**). Additionally, in GEO datasets, *SPATA20* expression was also lower in tumor than in normal tissue (**Figure 8C**). To validate this public data, IHC analysis was performed on a tumor microarray containing 59 tissue sections from patients with colorectal cancer. While SPATA20 was highly expressed in normal tissue, it was downregulated in primary and metastatic tumor tissues (**Figure 8D** and **8E**). Furthermore, a Kaplan-Meier survival analysis of TCGA primary colorectal cancer samples revealed that low expression of SPATA20 correlates with a poor survival rate (**Figure 8F** and **8G**). Overall, these findings suggest a negative correlation between SPATA20 expression and the development and progression of colorectal cancer.

Discussion

Hypoxia is a commonly observed feature in solid cancers [36]. The hypoxic tumor microenvironment can induce resistance to conventional chemotherapeutic agents [37-39]. Currently, targeting the HIF-1α pathway is being investigated as a novel therapeutic option for specific types of cancers linked to hypoxia [3, 40-42]. In this study, we present SPATA20 as a novel upstream regulator of HIF-1α that could potentially be used as a therapeutic and prognostic biomarker for hypoxia-driven cancers.

Although SPATA20 has been reported to be associated with colorectal cancer and cholangiocarcinoma, its biological function and role in cancer remain largely unknown [22, 23]. In previous studies, redox regulation of HIF-1α by the thioredoxin system has been investigated [18].
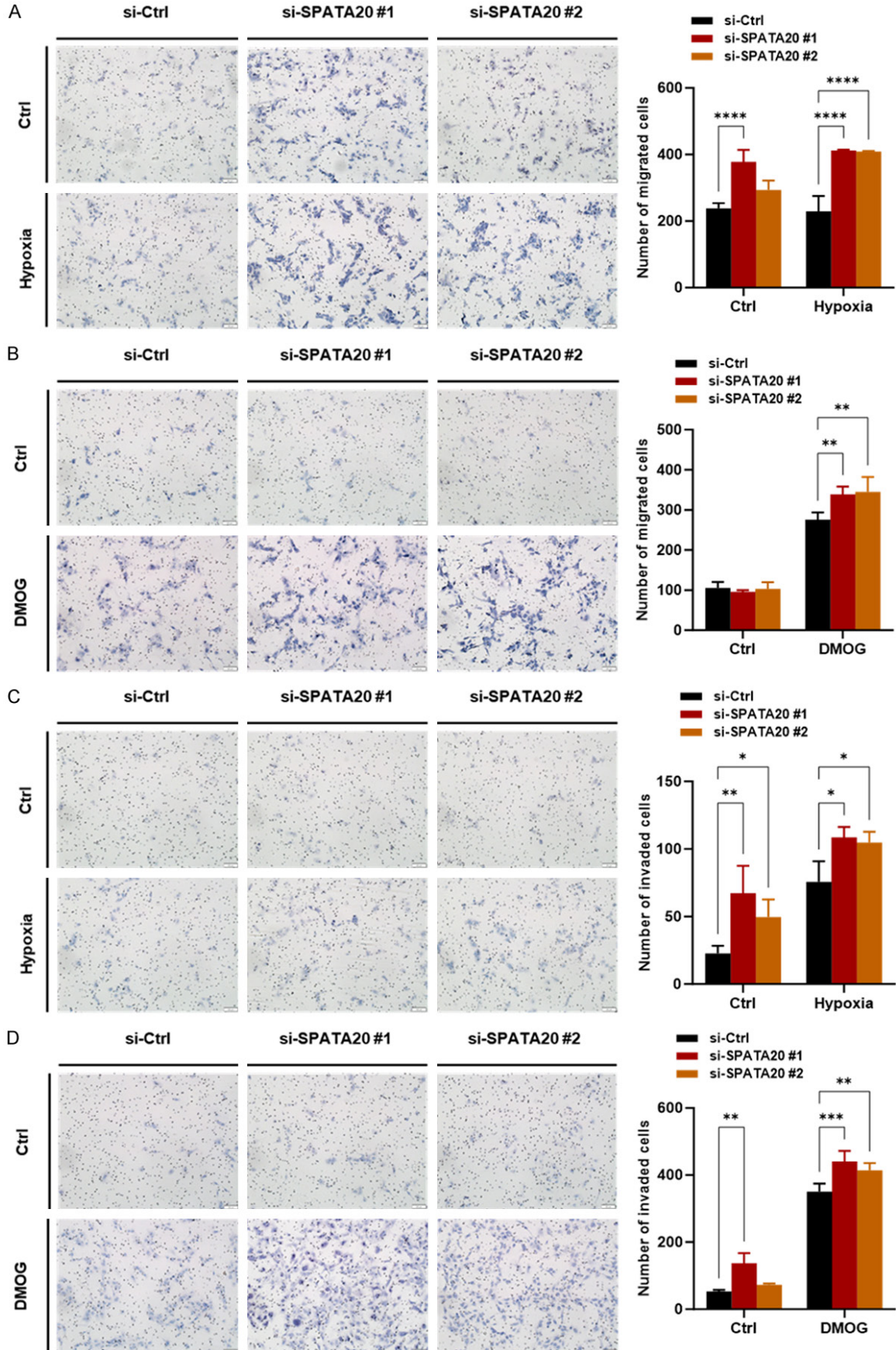
Figure 7. SPATA20 knockdown induces endothelial cell migration and invasion. (A, B) HUVECs were seeded in the upper chambers, and conditioned media collected from cancer cells transfected with the indicated siRNAs under hypoxia (A) or with 1 mM DMOG (B) were added to the lower chambers. Representative images of migrated cells are shown. The scale bars represent 100 μm. The average number of migrated cells was calculated from five random microscopic fields. (C, D) HUVECs were seeded in the upper chambers of BME-coated transwell inserts, and conditioned media collected from cells transfected with the indicated siRNAs under hypoxia (C) or with 1 mM DMOG (D) were added to the lower chambers. Representative images of invaded cells are shown. The average number of invaded cells was calculated from five random microscopic fields. Data are presented as means and SDs (n = 3). $*P < 0.05$, $**P < 0.01$, $***P < 0.001$, and $****P < 0.0001$ by two-way ANOVA.

As SPATA20 is a member of the thioredoxin-like fold proteins, which possesses a potential catalytic motif, it was anticipated that this domain might play an key role in regulating HIF-1α by controlling its redox status [18]. However, no evidence was found to suggest a direct interaction between HIF-1α and SPATA20. In fact, SPATA20 appears to function as an inhibitor of cap-dependent translation of HIF-1α. Our data suggest that SPATA20 indirectly regulates HIF-1α by controlling the phosphorylation of AKT at Ser473, which is involved in the translation process of HIF-1α. Further research is necessary to clarify whether SPATA20 exhibits redox activity and modulates HIF-1α through AKT in a redox-dependent manner.

In our experimental settings, while knockdown of SPATA20 successfully induced HIF-1α, ectopic expression of SPATA20 did not alter the expression of HIF-1α. This suggests that SPATA20 may require additional factors for its activity on HIF-1α, or it may need to form a protein complex to effectively bind and regulate HIF-1α. Thioredoxin reductases are integral parts of the thioredoxin system that reduce oxidized thioredoxin proteins by transferring electrons [43]. This system maintains redox homeostasis in cells, and thioredoxin reductases and thioredoxin proteins have a complementary relationship in its regulation. Therefore, it is possible that SPATA20 may require a specific thioredoxin reductase as a partner for the proper redox regulation of HIF-1α, if it has such activities. Identifying potential SPATA20-interacting proteins that are involved for HIF-1α regulation would be of research interest. Further investigation is required for a more comprehensive understanding of SPATA20 as an upstream regulator of HIF-1α.

The role of SPATA20 in human diseases, aside from sperm disorders, has been limited [20, 44]. However, it has been demonstrated that SPATA20 could serve as a biomarker for the early detection of cholangiocarcinoma [22]. More recently, mutations in SPATA20 have been implicated in the development of early-onset colorectal cancer [23]. In the current study, we discovered that the expression of SPATA20 is low in colorectal cancer through the analysis of public data and IHC of patient tissue samples. Furthermore, SPATA20 expression was found to be reduced in metastatic cancer compared to primary cancer. We verified that SPATA20-deficient cancer cells exhibited enhanced metastatic and angiogenic activities. These activities appear to be mediated, at least partially, through the activation of the HIF-1α pathway. HIF-1α inhibitors, such as YC-1, may have anti-cancer effects in SPATA20-deficient patients. Currently, several HIF-1α inhibitors are undergoing clinical trials for different types of cancer, and SPATA20 could be investigated as a potential indicator for HIF-1α-target therapy [45].

In conclusion, while previous studies on the function of SPATA20 were primarily focused on the male reproductive system, our study has revealed a novel role of SPATA20 in regulating the expression of HIF-1α in cancer. Developing SPATA20 as a biomarker for HIF-1α-targeting therapy may be an attractive strategy for treating patients with hypoxia-driven cancers.
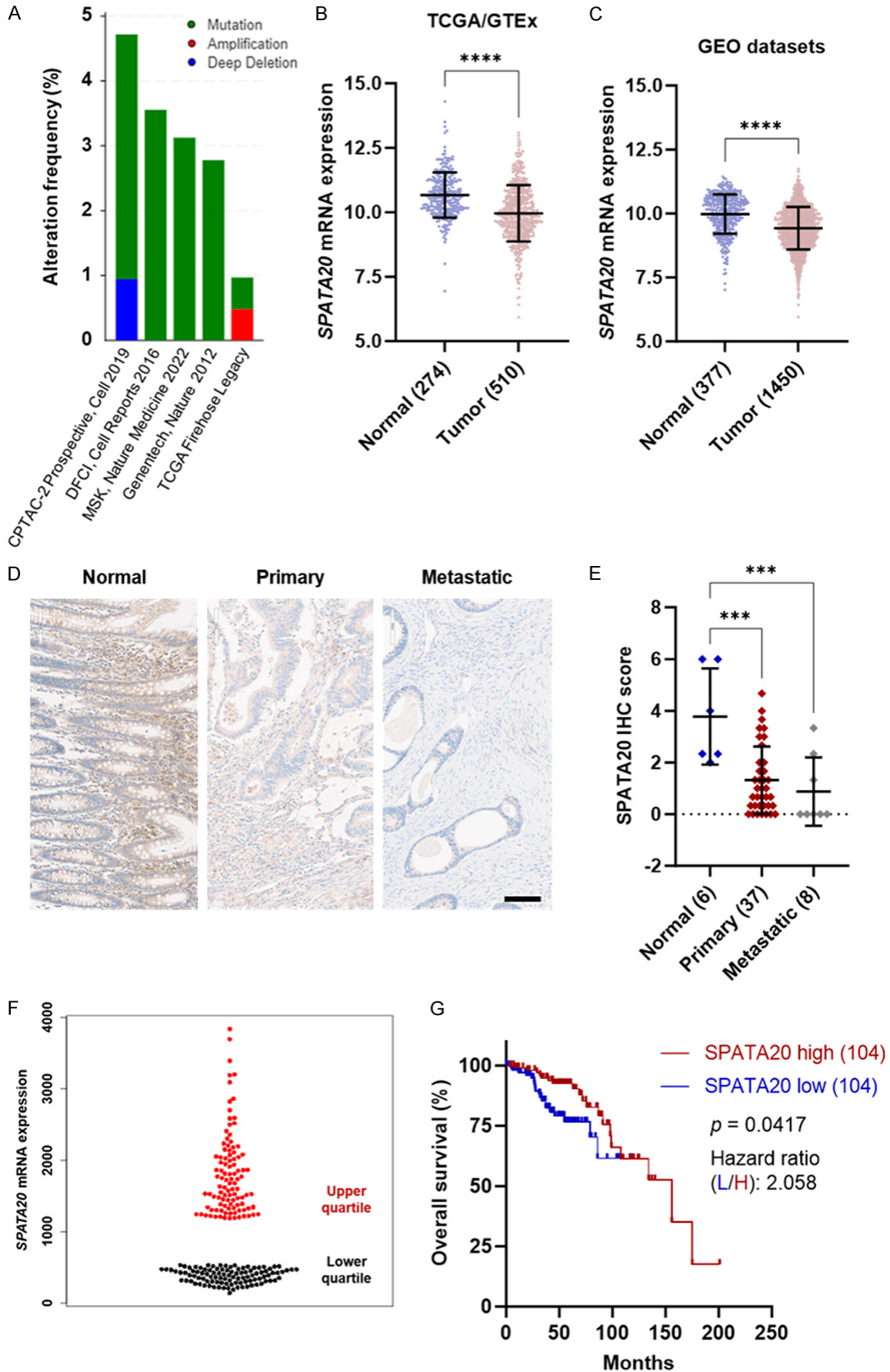
Acknowledgements

Disclosure of conflict of interest

None.

Address correspondence to: Dr. Iljin Kim, Department of Pharmacology and Program in Biomedical Science and Engineering, Inha University College of Medicine, 100 Inha-ro, Incheon 22212, South Korea. E-mail: ijk@inha.ac.kr

Figure 8. SPATA20 negatively correlates with colorectal cancer progression. (A) Genetic alteration frequencies in the *SPATA20* gene were analyzed in the cBioPortal platform, utilizing publicly available colorectal cancer datasets from multiple institutions. (B, C) *SPATA20* mRNA expression levels in normal and tumor tissues were assessed by utilizing RNA-seq and gene chip data from TCGA/GTEx (B) and GEO samples (C) in the TNMplot database. ****$P <$ 0.0001 by Mann-Whitney test. (D) A tumor microarray slide containing normal, primary tumor, and metastatic tumor tissues was analyzed by IHC staining using an anti-SPATA20 antibody. (E) The IHC score of SPATA20 was evaluated by multiplying the staining intensity by the percentage of positive cells. ***$P <$ 0.001 and ****$P <$ 0.0001 by one-way ANOVA. (F) Primary colorectal cancer samples from the TCGA dataset were divided into SPATA20 high (upper quartile) and low (lower quartile) groups according to the RNA-seq values. (G) Kaplan-Meier overall survival curves were plotted for the SPATA20 high and low groups. The *p*-value was analyzed using the log-rank test, and the hazard ratio was estimated using the Mantel-Haenszel method.

References

[1] Semenza GL. HIF-1 and mechanisms of hypoxia sensing. Curr Opin Cell Biol 2001; 13: 167-171.

[2] Cao D, Hou M, Guan YS, Jiang M, Yang Y and Gou HF. Expression of HIF-1alpha and VEGF in colorectal cancer: association with clinical outcomes and prognostic implications. BMC Cancer 2009; 9: 432.

[3] Jing X, Yang F, Shao C, Wei K, Xie M, Shen H and Shu Y. Role of hypoxia in cancer therapy by regulating the tumor microenvironment. Mol Cancer 2019; 18: 157.

[4] Fallah J and Rini BI. HIF inhibitors: status of current clinical development. Curr Oncol Rep 2019; 21: 6.

[5] Semenza GL. Hypoxia-inducible factor 1 (HIF-1) pathway. Sci STKE 2007; 2007: cm8.

[6] Koyasu S, Kobayashi M, Goto Y, Hiraoka M and Harada H. Regulatory mechanisms of hypoxia-inducible factor 1 activity: two decades of knowledge. Cancer Sci 2018; 109: 560-571.

[7] Kaelin WG. Proline hydroxylation and gene expression. Annu Rev Biochem 2005; 74: 115-128.

[8] Tirpe AA, Gulei D, Ciortea SM, Crivii C and Berindan-Neagoe I. Hypoxia: overview on hypoxia-mediated mechanisms with a focus on the role of HIF genes. Int J Mol Sci 2019; 20: 6140.

[9] Suzuki N, Gradin K, Poellinger L and Yamamoto M. Regulation of hypoxia-inducible gene expression after HIF activation. Exp Cell Res 2017; 356: 182-186.

[10] Welsh SJ, Bellamy WT, Briehl MM and Powis G. The redox protein thioredoxin-1 (Trx-1) increases hypoxia-inducible factor 1alpha protein expression: Trx-1 overexpression results in increased vascular endothelial growth factor production and enhanced tumor angiogenesis. Cancer Res 2002; 62: 5089-5095.

[11] Huang LE, Arany Z, Livingston DM and Bunn HF. Activation of hypoxia-inducible transcription factor depends primarily upon redox-sensitive stabilization of its alpha subunit. J Biol Chem 1996; 271: 32253-32259.

[12] Welsh SJ, Williams RR, Birmingham A, Newman DJ, Kirkpatrick DL and Powis G. The thioredoxin redox inhibitors 1-methylpropyl 2-imidazolyl disulfide and pleurotin inhibit hypoxia-induced factor 1alpha and vascular endothelial growth factor formation. Mol Cancer Ther 2003; 2: 235-243.

[13] Welsh S, Williams R, Kirkpatrick L, Paine-Murrieta G and Powis G. Antitumor activity and pharmacodynamic properties of PX-478, an inhibitor of hypoxia-inducible factor-1alpha. Mol Cancer Ther 2004; 3: 233-244.

[14] Zhou J, Damdimopoulos AE, Spyrou G and Brüne B. Thioredoxin 1 and thioredoxin 2 have opposed regulatory functions on hypoxia-inducible factor-1alpha. J Biol Chem 2007; 282: 7482-7490.

[15] Kobayashi Y, Oguro A, Hirata Y and Imaoka S. The regulation of hypoxia-inducible factor-1 (HIF-1alpha) expression by protein disulfide isomerase (PDI). PLoS One 2021; 16: e0246531.

[16] Lando D, Pongratz I, Poellinger L and Whitelaw ML. A redox mechanism controls differential DNA binding activities of hypoxia-inducible factor (HIF) 1alpha and the HIF-like factor. J Biol Chem 2000; 275: 4618-4627.

[17] Samanta D and Semenza GL. Maintenance of redox homeostasis by hypoxia-inducible factors. Redox Biol 2017; 13: 331-335.

[18] Shi HJ, Wu AZ, Santos M, Feng ZM, Huang L, Chen YM, Zhu K and Chen CL. Cloning and characterization of rat spermatid protein SSP411: a thioredoxin-like protein. J Androl 2004; 25: 479-493.

[19] Liu M, Ru Y, Gu Y, Tang J, Zhang T, Wu J, Yu F, Yuan Y, Xu C, Wang J and Shi H. Disruption of Ssp411 causes impaired sperm head formation and male sterility in mice. Biochim Biophys Acta Gen Subj 2018; 1862: 660-668.

[20] Martinez G, Metzler-Guillemain C, Cazin C, Kherraf ZE, Paulmyer-Lacroix O, Arnoult C, Ray PF and Coutton C. Expanding the sperm phenotype caused by mutations in SPATA20: a novel splicing mutation in an infertile patient with partial globozoospermia. Clin Genet 2023; 103: 612-614.

[21] Omolaoye TS, Hachim MY and du Plessis SS. Using publicly available transcriptomic data to identify mechanistic and diagnostic biomarkers in azoospermia and overall male infertility. Sci Rep 2022; 12: 2584.

[22] Shen J, Wang W, Wu J, Feng B, Chen W, Wang M, Tang J, Wang F, Cheng F, Pu L, Tang Q, Wang X and Li X. Comparative proteomic profiling of human bile reveals SSP411 as a novel biomarker of cholangiocarcinoma. PLoS One 2012; 7: e47476.

[23] Fernández-Rozadilla C, Álvarez-Barona M, Quintana I, López-Novo A, Amigo J, Cameselle-Teijeiro JM, Roman E, Gonzalez D, Llor X, Bujanda L, Bessa X, Jover R, Balaguer F, Castells A, Castellví-Bel S, Capellá G, Carracedo A, Valle L and Ruiz-Ponte C. Exome sequencing of early-onset patients supports genetic heterogeneity in colorectal cancer. Sci Rep 2021; 11: 11135.

[24] Choi YJ, Kim I, Lee JE and Park JW. PIN1 transcript variant 2 acts as a long non-coding RNA that controls the HIF-1-driven hypoxic response. Sci Rep 2019; 9: 10599.

[25] Chun YS, Choi E, Yeo EJ, Lee JH, Kim MS and Park JW. A new HIF-1 alpha variant induced by zinc ion suppresses HIF-1-mediated hypoxic responses. J Cell Sci 2001; 114: 4051-4061.

[26] Chun YS, Choi E, Kim GT, Lee MJ, Lee MJ, Lee SE, Kim MS and Park JW. Zinc induces the accumulation of hypoxia-inducible factor (HIF)-1alpha, but inhibits the nuclear translocation of HIF-1beta, causing HIF-1 inactivation. Biochem Biophys Res Commun 2000; 268: 652-656.

[27] Naranjo-Suarez S, Carlson BA, Tobe R, Yoo MH, Tsuji PA, Gladyshev VN and Hatfield DL. Regulation of HIF-1α activity by overexpression of thioredoxin is independent of thioredoxin reductase status. Mol Cells 2013; 36: 151-157.

[28] ICGC/TCGA Pan-Cancer Analysis of Whole Genomes Consortium. Pan-cancer analysis of whole genomes. Nature 2020; 578: 82-93.

[29] Kim I and Park JW. Hypoxia-driven epigenetic regulation in cancer progression: a focus on histone methylation and its modifying enzymes. Cancer Lett 2020; 489: 41-49.

[30] Pore N, Jiang Z, Shu HK, Bernhard E, Kao GD and Maity A. Akt1 activation can augment hypoxia-inducible factor-1alpha expression by increasing protein translation through a mammalian target of rapamycin-independent pathway. Mol Cancer Res 2006; 4: 471-479.

[31] Biller LH and Schrag D. Diagnosis and treatment of metastatic colorectal cancer: a review. JAMA 2021; 325: 669-685.

[32] Riihimäki M, Thomsen H, Hemminki A, Sundquist K and Hemminki K. Comparison of survival of patients with metastases from known versus unknown primaries: survival in metastatic cancer. BMC Cancer 2013; 13: 36.

[33] Liu ZJ, Semenza GL and Zhang HF. Hypoxia-inducible factor 1 and breast cancer metastasis. J Zhejiang Univ Sci B 2015; 16: 32-43.

[34] Ghoshal P, Teng Y, Lesoon LA and Cowell JK. HIF1A induces expression of the WASF3 metastasis-associated gene under hypoxic conditions. Int J Cancer 2012; 131: E905-915.

[35] Krock BL, Skuli N and Simon MC. Hypoxia-induced angiogenesis: good and evil. Genes Cancer 2011; 2: 1117-1133.

[36] Semenza GL. Targeting HIF-1 for cancer therapy. Nat Rev Cancer 2003; 3: 721-732.

[37] Schirrmacher V. From chemotherapy to biological therapy: a review of novel concepts to reduce the side effects of systemic cancer treatment (Review). Int J Oncol 2019; 54: 407-419.

[38] Dasari S and Tchounwou PB. Cisplatin in cancer therapy: molecular mechanisms of action. Eur J Pharmacol 2014; 740: 364-378.

[39] Alonso Castellanos S, Soto Célix M, Alonso Galarreta J, del Riego Valledor A and Miján de la Torre A. Associated metabolic and nutritional side effects to biological cancer therapy. Nutr Hosp 2014; 29: 259-268.

[40] Patel A and Sant S. Hypoxic tumor microenvironment: Opportunities to develop targeted therapies. Biotechnol Adv 2016; 34: 803-812.

[41] Jeon S, Jeon M, Choi S, Yoo S, Park S, Lee M and Kim I. Hypoxia in skin cancer: molecular basis and clinical implications. Int J Mol Sci 2023; 24: 4430.

[42] Semenza GL. Pharmacologic targeting of hypoxia-inducible factors. Annu Rev Pharmacol Toxicol 2019; 59: 379-403.

[43] Lu J and Holmgren A. The thioredoxin antioxidant system. Free Radic Biol Med 2014; 66: 75-87.

[44] Wang X, Jiang C, Dai S, Shen G, Yang Y and Shen Y. Identification of nonfunctional SPATA20 causing acephalic spermatozoa syndrome in humans. Clin Genet 2023; 103: 310-319.

[45] Wigerup C, Pahlman S and Bexell D. Therapeutic targeting of hypoxia and hypoxia-inducible factors in cancer. Pharmacol Ther 2016; 164: 152-169.

Supplementary Table 1. List of siRNAs

Name	Sequence (5'-3')
Ctrl	UUGAGCAAUUCACGUUCAUTT
SPATA20 #1	AGGUGAAGCAUCCCAACUGACUAGA
SPATA20 #2	GUGUUGCUGAGAAUACGAGAACAGT

Supplementary Table 2. List of primers used in RT-qPCR

| Name	Sequence (5'-3')
EDN1	Forward: CTACTTCTGCCACCTGGACATC Reverse: TCACGGTCTGTTGCCTTTGTGG
PLAU	Forward: GGCTTAACTCCAACACGCAAGG Reverse: CCTCCTTGGAACGGATCTTCAG
HMOX1	Forward: CCAGGCAGAGAATGCTGAGTTC Reverse: AAGACTGGGCTCTCCTTGTTGC
ADM	Forward: GACATGAAGGGTGCCTCTCGAA Reverse: CCTGGAAGTTGTTCATGCTCTGG
HIF1A	Forward: TATGAGCCAGAAGAACTTTTAGGC Reverse: CACCTCTTTTGGCAAGCATCCTG
HIF1A pre-mRNA	Forward: GTCTGCGAGAAAACTTTGTAA Reverse: ATGTGTGCATTTTACCTGAGT
ACTB	Forward: CACCATTGGCAATGAGCGGTTC Reverse: AGGTCTTTGCGGATGTCCACGT
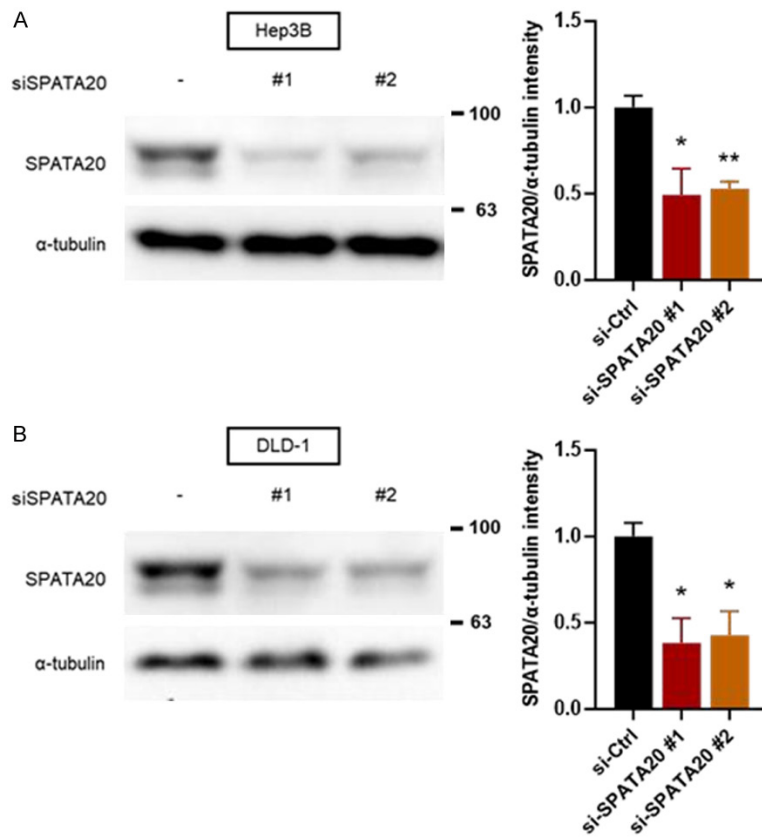
Supplementary Figure 1. Cells were transfected with indicated siRNAs and analyzed by Western blotting. The bar graphs display the band intensities of SPATA20 protein normalized to the intensities of α-tubulin. Data are presented as means and SDs (n = 3).
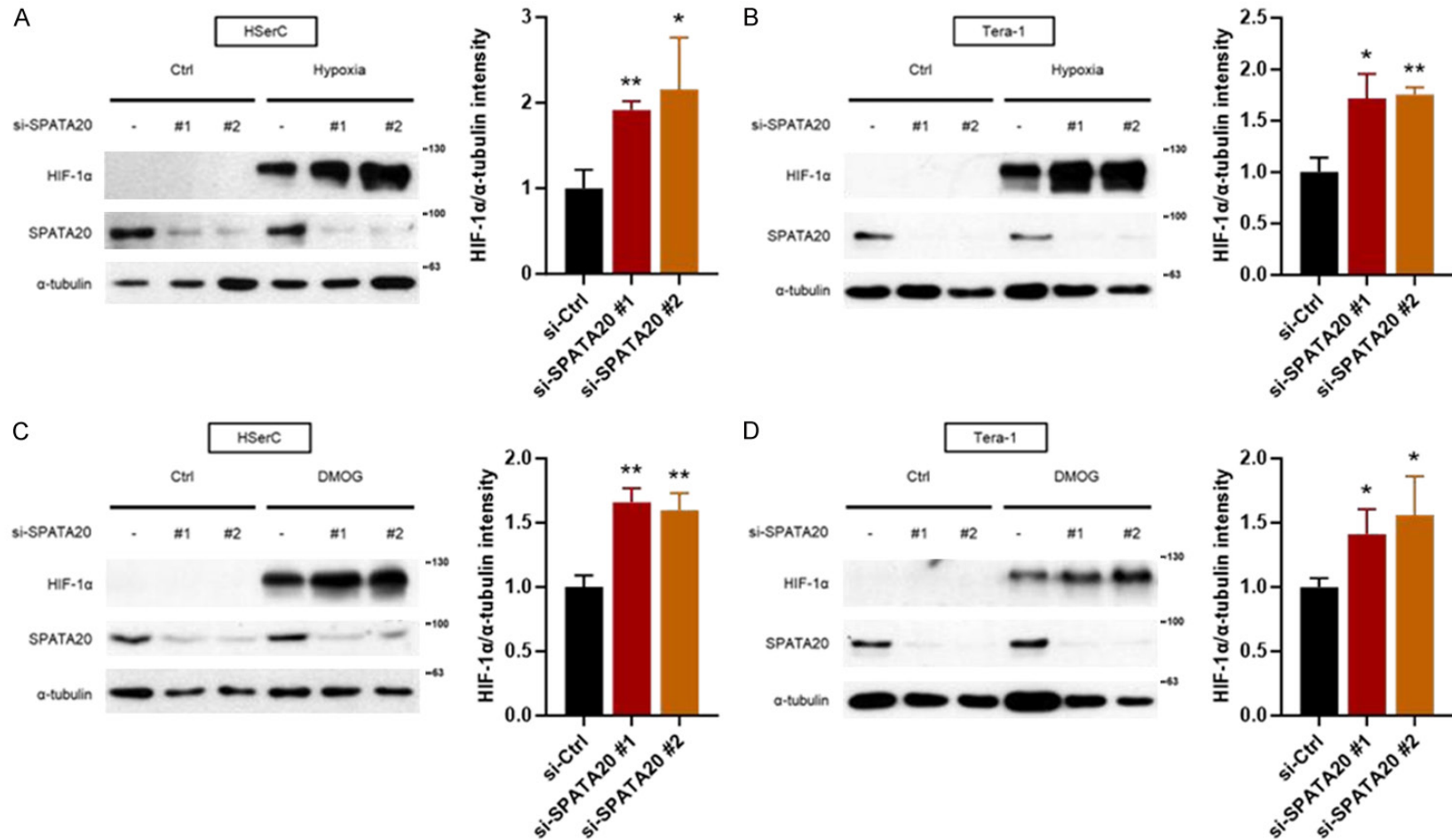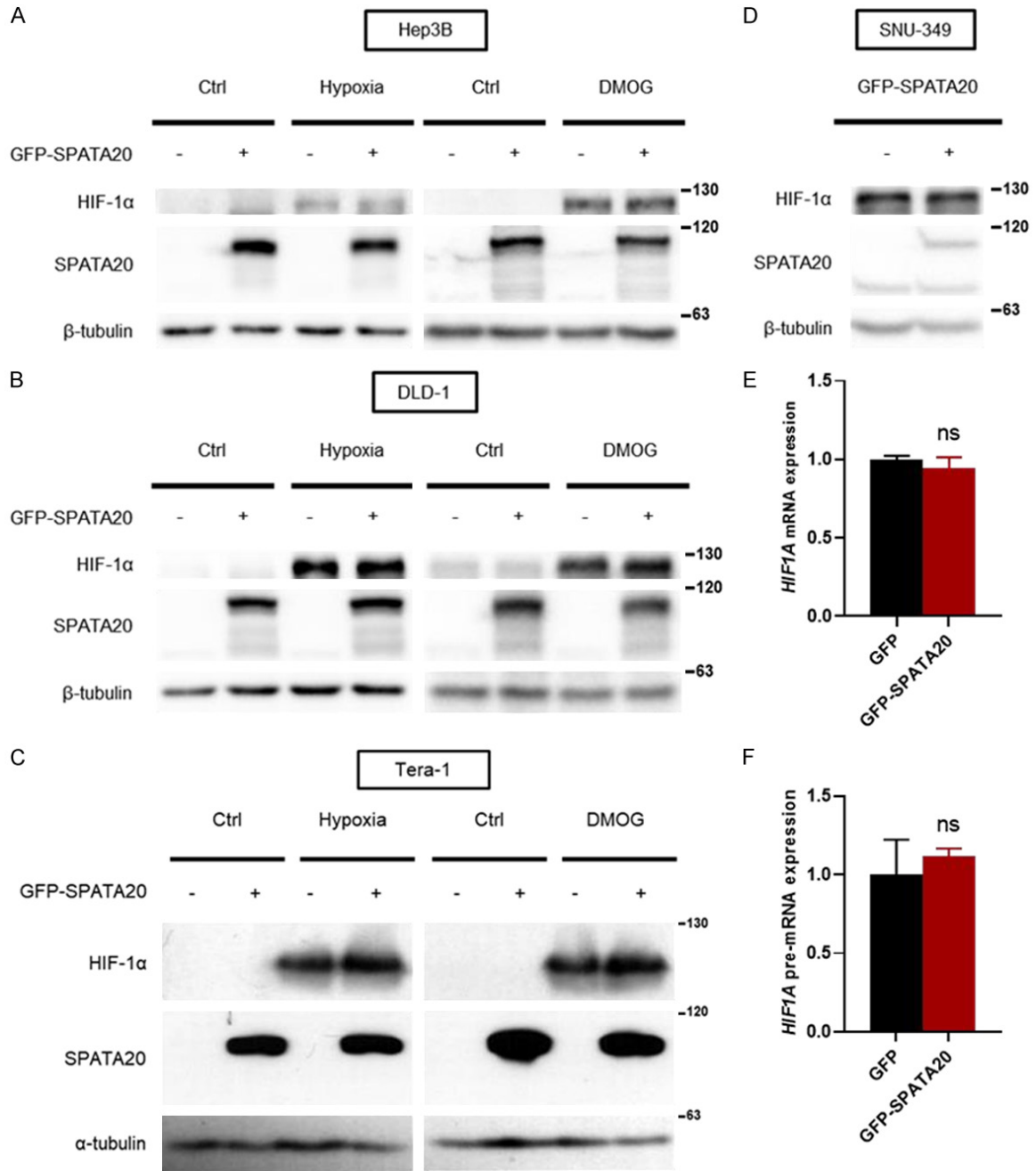
Supplementary Figure 2. HSerC and Tera-1 cells were transfected with indicated siRNAs and incubated in hypoxia (A, B) or treated with 1 mM DMOG (C, D) for 8 hours. Cell lysates were analyzed by Western blotting with the indicated antibodies. The bar graphs display the band intensities of HIF-1α protein normalized to the intensities of α-tubulin in the hypoxia or DMOG groups. Data are presented as means and SDs (n = 3). *P < 0.05 and **P < 0.01 compared to the si-Ctrl groups by Student's t-test.
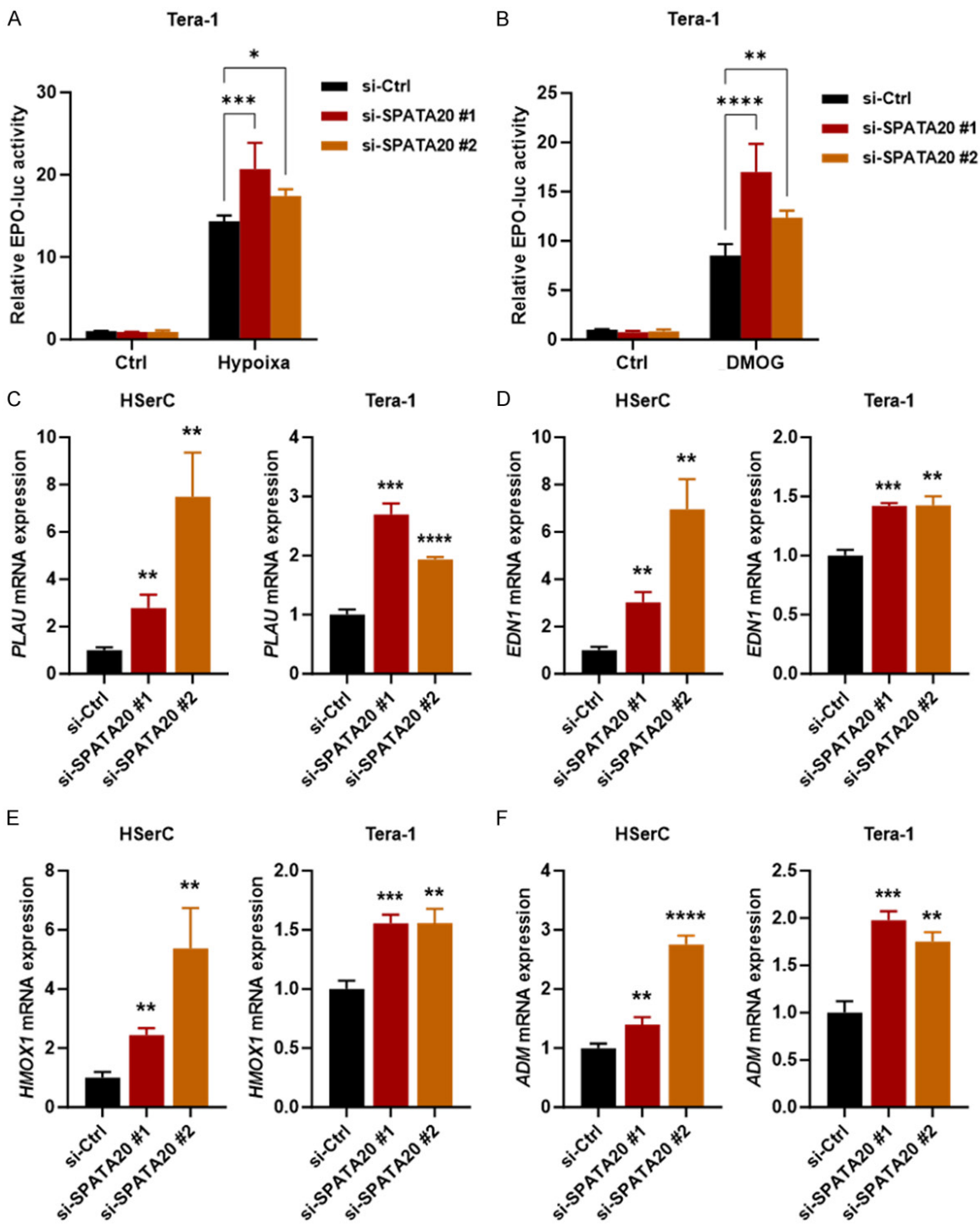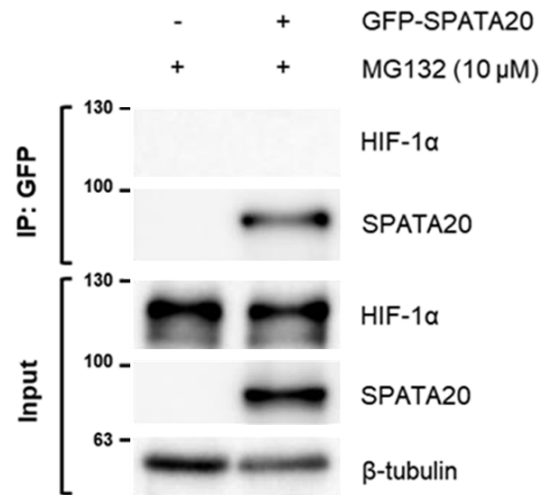
Supplementary Figure 3. (A, B) Tera-1 cells were transfected with EPO-luciferase plasmid and indicated siRNAs and then incubated in hypoxia (A) or treated with 1 mM DMOG (B) for 24 hours. Cells were lysed and subjected to the luciferase assay. Data represents the mean ± SD (n = 3). *$P < 0.05$, **$P < 0.01$, ***$P < 0.001$ and ****$P < 0.0001$ by two-way ANOVA. (C-F) Cells were transfected with indicated siRNAs and cultured in hypoxia for 24 hours. Cells were lysed for RNA extraction, and the mRNA expression levels of *PLAU* (C), *EDN1* (D), *HMOX1* (E), and *ADM* (F) were measured by RT-qPCR. Relative expression levels were determined by normalizing to *ACTB* expression levels. Data represents the mean ± SD (n = 3). **$P < 0.01$, ***$P < 0.001$, and ****$P < 0.0001$ compared to the si-Ctrl groups by Student's t-test.
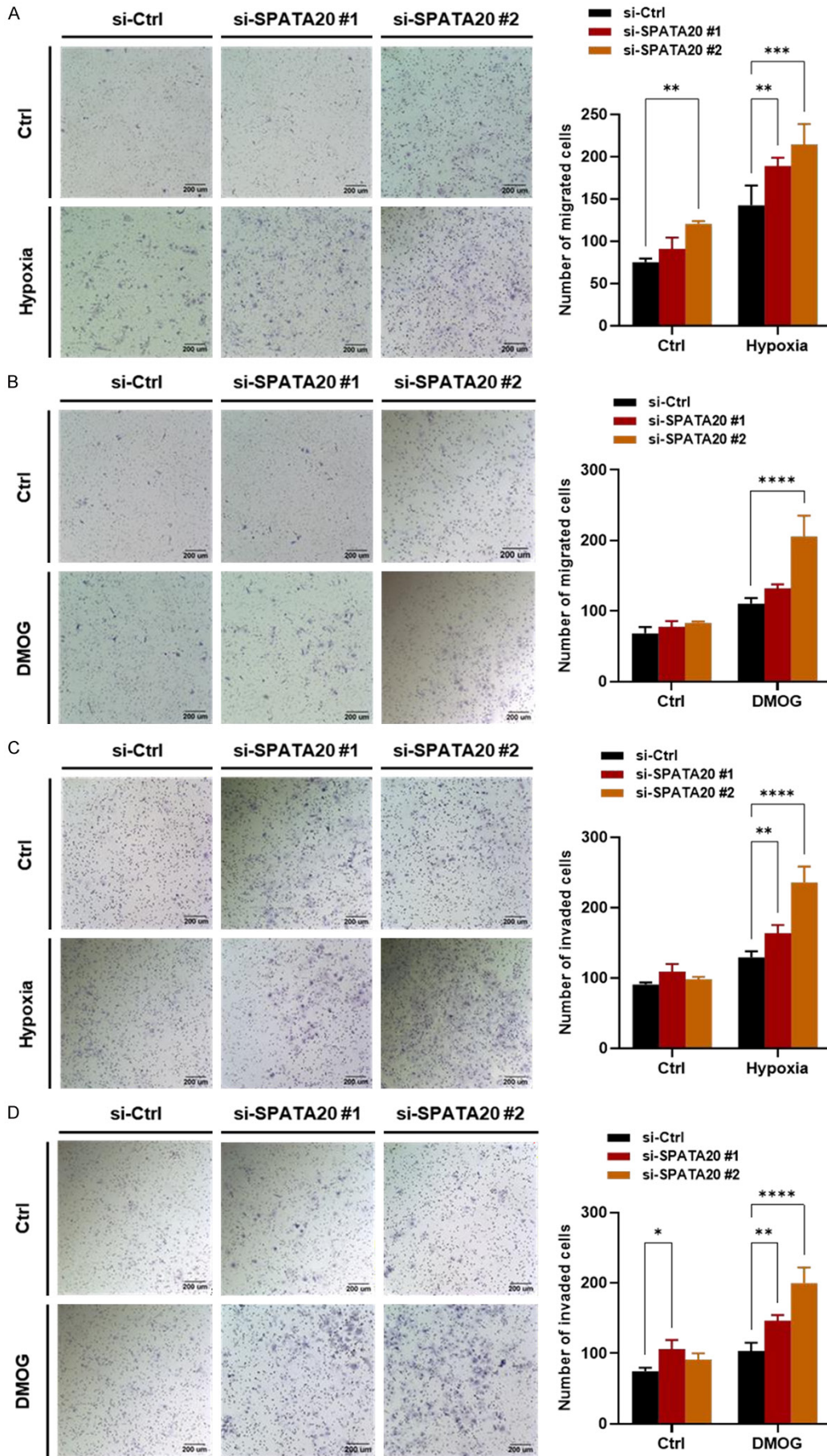
Supplementary Figure 4. (A-C) Hep3B, DLD-1, Tera-1 cells were transfected with GFPor GFP-SPATA20 plasmid and incubated in hypoxia or treated with 1 mM DMOG for 8 hours. Cell lysates were analyzed by Western blotting using the indicated antibodies. (D) *VHL*-mutant SNU-349 cells were transfected with GFP or GFP-SPATA20 plasmid and analyzed by Western blotting. (E, F) Hep3B cells were transfected with GFP or GFP- SPATA20 plasmid and lysed for RNA extraction. *HIF1A* mRNA (E) and pre-mRNA (F) expression levels were measured by RT-qPCR. Data are presented as means and SDs (n = 3). ns, non-significant ($P > 0.05$ by Student's t-test).

HIF-1α regulation by SPATA20

Supplementary Figure 5. Cells were transfected with GFP-tagged SPATA20 and thentreated with 10 μM MG132 for 6 hours. The resulting cell lysates were subjected to immunoprecipitation (IP) using an anti-GFP antibody. Cell lysates and precipitatedsamples were analyzed by Western blotting.

Supplementary Figure 6. (A, B) Hep3B cells were transfected with indicated siRNAs and subjected to transwell migration assays under hypoxia (A) or with 1 mM DMOG (B) added to the lower chambers. Representative images of migrated cells are shown. The scale bars represent 200 μm. The average number of migrated cells was calculated from five random microscopic fields. (C, D) Cells were transfected with the indicated siRNAs and subjected to invasion assays under hypoxia (C) or with 1 mM DMOG (D) added to the lower chambers. Representative images of invaded cells are shown. The average number of invaded cells was calculated from five random microscopic fields. Data are presented as means and SDs (n = 3). *P < 0.05, **P < 0.01, ***P < 0.001, and ****P < 0.0001 by two-way ANOVA with Dunnett's multiple comparisons test.
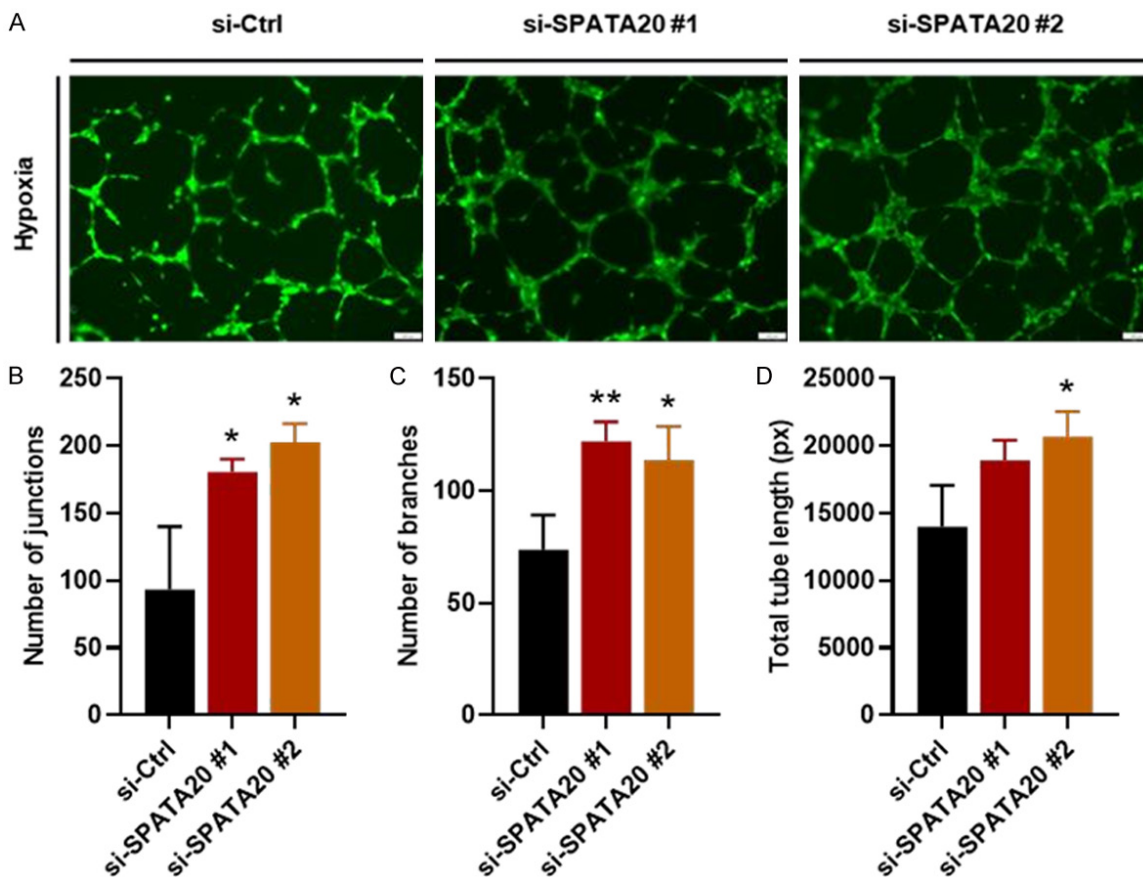
Supplementary Figure 7. SPATA20 knockdown enhances the angiogenic potential of endothelial cells. (A) HUVECs were seeded onto basement membrane extract-coated wells and cultured with conditioned media collected from cancer cells transfected with the indicated siRNAs under hypoxia. Representative images of tube formation are shown. (B-D) Tubular networks were analyzed in random microscopic fields using the Angiogenesis Analyzer ImageJ plugin program. The number of junctions (B), branches (C), and total tube length (D) were analyzed. Data are presented as means and SDs (n = 3). *P < 0.05 and **P < 0.01 by Student's t-test.